ISSN 2229-5518

Modeling of Quadruplex BLDC Motor Actuator Based Position Servo System

Minnu Jayan C

Abstract— The paper describes Quadruplex Brushless DC motor based actuator in a position servo system. In the aerospace applications Electro Mechanical Actuators (EMA) are mainly used in the flight control system of aircrafts, missiles or launch vehicles as it is relatively compact and can offer high power to weight ratios and motion velocities. Quadruplex BLDC motors provide very high redundancy for the actuator. The work aims to develop the model of a new genre of Quadruplex BLDC motors presently used in launch vehicle application. An inverter is designed to provide phase voltages in order to drive the motor. Current controller senses the rotor position and generates gating pulses to switch the inverter. Load dynamics is designed to function as an EMA. Finally position controller is tuned to track the position of a launch vehicle. Thus closed loop position control system is explained. In order to model the BLDC motors, parameter values are selected based on the specification. The modeling of BLDC motor is done in state-space. It offers flexibility and easiness in implementation. An FDI system is included in the system to improve the efficiency. So that if any fault occurs, it will be detected, isolated and a redundant system will work. The simulation results are presented by using MATLAB/SIMULINK as the simulation tool.

Index Terms— Electromechanical actuator (EMA), Quadruplex BLDC Motor, Commutation, Position Servo System, Compensator, Fault Detection and Isolation (FDI) MATLAB

1 INTRODUCTION

Due to the development in engineering and material technology, tremendous improvement in solid state devices and circuits, new types of electric motors like stepper motors, switched reluctance motors and permanent magnet motors have emerged. Out of these, the Permanent Magnet Brushless DC [PMBLDC] motors, is the second stage evolution of conventional dc motor [12]. To improve reliability and robustness, Brushless DC (BLDC) motors have been used nowadays. The main difference in construction of the PMBLDC motor from conventional dc motor is the stator poles. They are replaced by suitable permanent magnets. Because of the presence of permanent magnet in PMBLDC motors, there is no need to have field windings. Torque is generated by the interaction of stator poles and permanent magnets. In order to discharge a satellite into the desired orbit, the launch vehicle has to follow a definite path which is termed the trajectory. The aim of keeping the launch vehicle in the trajectory path can be made into possible by controlling its movement.

This can be done by controlling the position of nozzle of the vehicle. The position of the nozzle can be controlled by means of actuators. Usually Electromechanical and Electro hydraulic actuators are used for this purpose. But electromechanical actuators (EMAs) are having several advantages over all Electro Hydraulic actuators. Of the various kinds of actuators, EMAs were chosen because of their growing role in the aerospace field, from civilian airliners to robotic spacecraft.

They gain importance as it is cheap, operation is automated, possibility of position feedback. Traditional DC motors are limited in reliability and robustness due to wear of the brush and commutation mechanisms. Actuators are safety-critical components of an aerospace system and an undetected actuator failure can lead to serious consequences. They are relatively compact and can offer high power to Weight ratios and motion velocities. Advantages of BLDC motors include - Better Speed-Torque characteristics, High Dynamic Response, High Efficiency, Long operating life, Noiseless operation, higher speed ranges [5].

Commutation is the process of switching currents from one winding to another. It helps rotation of the motor in either direction [19]. Commutation employed in the paper is the trapezoidal commutation. Hall Effect Sensors are effective for rotor position sensing. It makes two power switching devices on each motor phase in a predetermined sequence. This is a simple control algorithm. It is very effective in controlling motor speed, torque ripple at low speed. The rotational motion from the BLDC motor is transferred to the ball screw by means of gearing systems. Thus the rotational motion is transferred to a proportional linear motion by ball screw.

An Electromechanical Actuation System with Dual Redundancy is composed of two main sub systems [2]. They are Prime Chain and Redundant chain. One is a closed loop position control system, which is termed the Prime chain for the Actuator which includes a motor which is a BLDC motor and a mechanical arrangement which is a ball screw .Second

- *Minnu Jayan C has pursued masters degree program in Applied Electronics in Anna University Chennai ,India,. E-mail:minnu.j@gmail.com*

International Journal of Scientific & Engineering Research, Volume 3, Issue 12, December-2012
ISSN 2229-5518

one, termed the Redundant chain is a Fault Detection and Isolation (FDI) system which detects and isolates the fault in the system by isolating the Prime chain which has the fault and switching to the redundant chain.

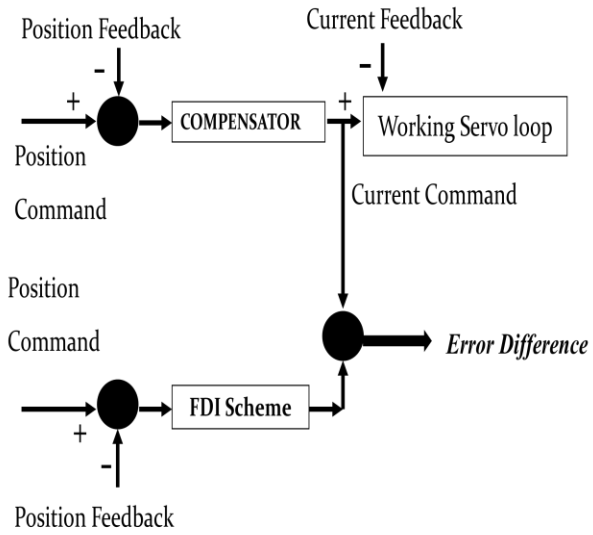

Fig. 1 Block Diagram of FDI Scheme

Due to high cost and criticality of mission, these systems are designed with a high degree of redundancy which involve both analytical and hardware redundancy. Hardware redundancy refers to ensuring reliability of the system by providing parallel hardware that can be alternatively switched on and bypass the system that turns faulty. Analytical redundancy refers to ensuring reasonable performance even in presence of fault by reconfiguring the system allowing a graceful degradation in performance. Both of these depend on the Fault Detection and Isolation (FDI) scheme which has to detect the occurrence of fault, pinpoint its location and the degree of fault (how much it affect its performance). Certain systems also predict how long the subsystem can give satisfactory performance even in presence of fault. If any fault occurs in the prime chain, the FDI Logic detects the fault, isolates the prime chain from the system and automatically switches to the redundant chain which controls the motor further [13]. This paper presents the modeling of BLDC motor and drive; closed loop position system modeling is explained. Also Failure detection and isolation conditions are analyzed by introducing an FDI Scheme. This is shown in Fig. 1.By verifying the error difference, the system switches to redundant chain. For modeling the BLDC motor, parameter values are selected based on the specification. The modeling of BLDC Motor is done in state-space. The design of the compensator for the system is also highlighted. The modeling is carried out in MATLAB/Simulink platform for which the results are presented.

2 MODELING OF OVERALL SYSTEM BASED ON MATLAB/SIMULINK

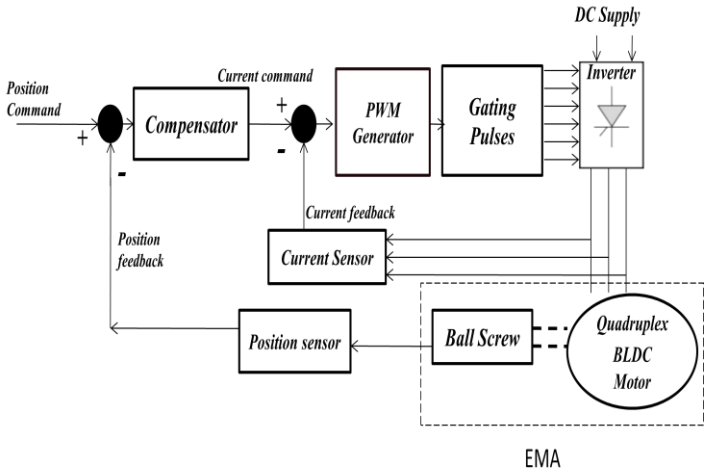

Fig. 2 Basic Block Diagram of Position Servo System

The block diagram of the overall system is shown in Fig. 2. It represents a closed loop position control of a BLDC motor system with an inner current control loop [6]. The position feedback which is sensed by a position sensor is fed back and compared with the position command signal. The error signal is given to the compensator system and its output forms the reference current, which may be called the current command. Current feedback obtained from the current sensor is compared with the current command. The compared output is used to generate the PWM signal in turn is fed to the gating pulse generation. The six gating signals are provided to the VSI which generates phase voltages in order to run the BLDC Motor.

The construction diagram of the simulated model is shown in Fig .3. This figure is a three phase six state Brushless DC Motor with Y-connected windings. The modeling of BLDCM is obtained by using State Space Analysis. The BLDCM produces a Trapezoidal back EMF (electro motive force) and rectangular shaped current waveforms [1].

International Journal of Scientific & Engineering Research, Volume 3, Issue 12, December-2012
ISSN 2229-5518

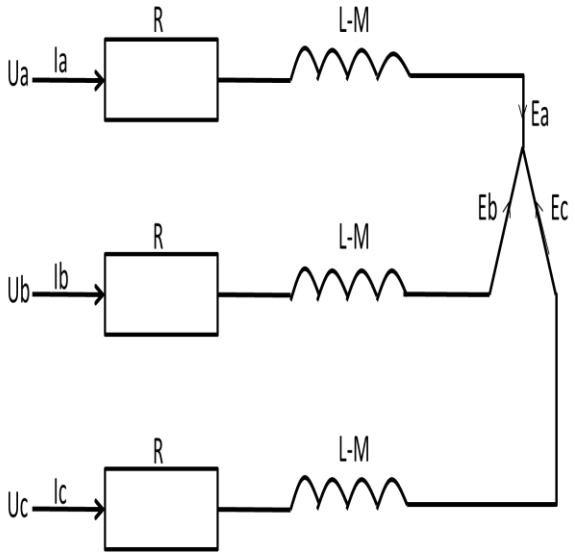

Fig. 3 Equivalent circuit for BLDCM

The following assumptions are made:

(1)The three phase windings are symmetrical.
(2)Magnetic Saturation is neglected.
(3)Eddy current and hysteresis losses are neglected.
(4)The resistance of each of the motor winding is considered as R, the self inductance is L and mutual inductance is M. Hence the three-phase stator voltage balance equation can be expressed by the following state equation as shown.

Taking Kirchoff's voltage law

$$Ua = Ra \times Ia + Laa\left(\frac{dIa}{dt}\right) + Lab\left(\frac{dIb}{dt}\right) + Lac\left(\frac{dIc}{dt}\right) + Ea \quad (1)$$

$$Ub = Rb \times Ib + Lba\left(\frac{dIa}{dt}\right) + Lbb\left(\frac{dIb}{dt}\right) + Lbc\left(\frac{dIc}{dt}\right) + Eb \quad (2)$$

$$Uc = Rc \times Ic + Lca\left(\frac{dIa}{dt}\right) + Lcb\left(\frac{dIb}{dt}\right) + Lcc\left(\frac{dIc}{dt}\right) + Ec \quad (3)$$

Self Inductance, $Laa, Lbb, Lcc = L$

Mutual Inductance, $Lab, Lac, Lba, Lbc, Lca, Lcb = M$

The stator phase currents are constrained to be balanced.

ie. $Ia + Ib + Ic = 0;$

Matrix equation is written as:

$$\begin{bmatrix} Ua \\ Ub \\ Uc \end{bmatrix} = \begin{bmatrix} R & 0 & 0 \\ 0 & R & 0 \\ 0 & 0 & R \end{bmatrix} + \begin{bmatrix} Ia \\ Ib \\ Ic \end{bmatrix} + \begin{bmatrix} L-M & 0 & 0 \\ 0 & L-M & 0 \\ 0 & 0 & L-M \end{bmatrix} \frac{d}{dt} \begin{bmatrix} Ia \\ Ib \\ Ic \end{bmatrix} + \begin{bmatrix} Ea \\ Eb \\ Ec \end{bmatrix}$$

The instantaneous induced EMFs are given as:

$$Ea = fa(\theta r) \times Ke \times wm \quad (4)$$

$$Eb = fb(\theta r) \times Ke \times wm \quad (5)$$

$$Ec = fc(\theta r) \times Ke \times wm \quad (6)$$

Where Ke is the back EMF constant

Torque equation is as follows,

$$T_e = Ke[f_a(\theta_r)I_a + f_b(\theta_r)I_b + f_c(\theta_r)I_c] \quad (7)$$

Where I_a, I_b, I_c are the stator currents.

The equation of motion for a simple system with inertia J, friction coefficient B and load torque T_l is,

$$J\frac{dwm}{dt} + B(wm) = T_e - T_l \quad (8)$$

Electrical rotor speed and position are related by

$$\frac{d\theta r}{dt} = \left(\frac{P}{2}\right) wm \quad (9)$$

Where, wm is rotor speed, J is moment of inertia

B is friction coefficient, T_l is Load Torque

T_e is Electrical Torque, P is No: of Poles

θ_r is rotor position

The system is represented in state space form as:

$X' = AX + BU$ (State Vector)

$Y = CX + DU$ (Output Vector)

Where, A is the State Matrix

B is the Input Matrix

C is the Output Matrix

D is the direct feed through Matrix

The state variable (θ_r), rotor position, requires a function $f_a(\theta_r)$, which is given as the trapezoidal function

$$\begin{aligned} f_a(\theta_r) &= 1 && 0 < \theta_r < {}^{\pi}/_{3} \\ &= \left(\frac{\pi}{2} - \theta_r\right)\frac{6}{\pi} && {}^{\pi}/_{3} < \theta_r < {}^{2\pi}/_{3} \\ &= -1 && {}^{2\pi}/_{3} < \theta_r < \pi \\ &= -1 && \pi < \theta_r < {}^{4\pi}/_{3} \\ &= \left(\theta_r - \frac{3\pi}{2}\right)\frac{6}{\pi} && {}^{4\pi}/_{3} < \theta_r < {}^{5\pi}/_{3} \\ &= 1 && {}^{5\pi}/_{3} < \theta_r < 2\pi \end{aligned} \quad (10)$$

International Journal of Scientific & Engineering Research, Volume 3, Issue 12, December-2012
ISSN 2229-5518

2.1 Modeling Of BLDCM

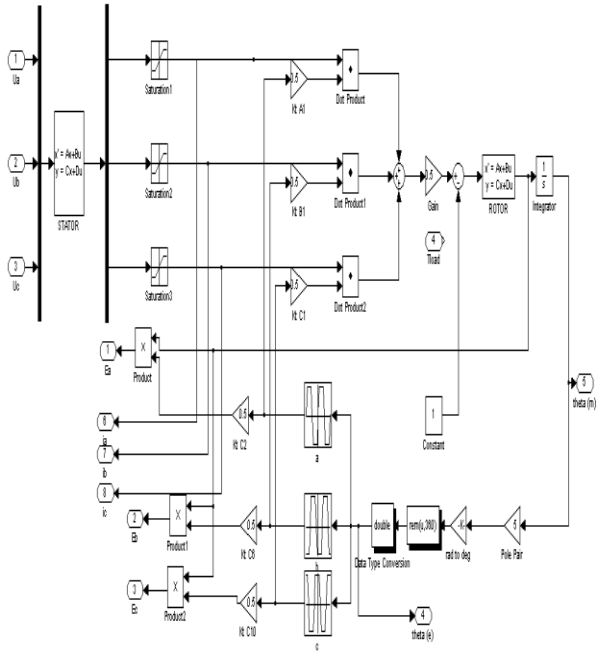

Fig. 4 Simulink model of BLDCM

Fig. 4 shows the mathematical model of BLDCM has been done in SIMULINK. The proposed model is developed based on the rotor reference frame of BLDCM. The model has a flexible structure and enables users to change motor parameters [8].Rotor and Stator part of the motor is separately modeled.

2.2 Modeling Of Drive

Six switch three phase modes, which is the voltage to source inverter, are being used [3]. Six gating signals are responsible for the switching of the upper and lower switches. Fig. 5(a) implies the inverter in the system is modeled by considering the conduction and commutation subinterval which is present between the switching. During conduction, the inverter divides the supply voltage equally between the two conducting phases. Fig. 5(b) describes the switching action of the inverters. One of the cases is illustrated with an example. When one of the switches in the inverter turns off, freewheeling action takes place that makes the corresponding phase current to reach zero [3],[4]. Output of the inverter produces phase voltages which help to drive the BLDCM. For convenience, the inverter logic modeled for the phase A is shown in Fig. 6. The same logic is then repeated for the other phases also. For the common 3-phase BLDC motor, a standard 3-phase power stage is used. The power stage utilizes six power transistors that operate in either an independent or complementary mode. In both modes, the 3-phase power stage energizes two motor phases concurrently. The third phase is unpowered. Thus, we get six possible voltage vectors that are applied to the BLDC motor using a Pulse Width Modulation (PWM) technique [4]. By energizing minimum number of motor phases, power requirement is reduced and there by cost and complexity is reduced.

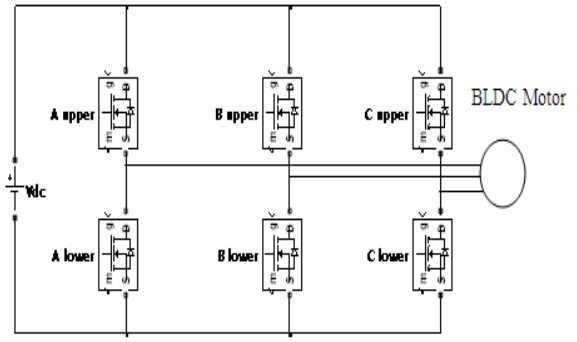

Fig. 5(a) Voltage to Source Inverter

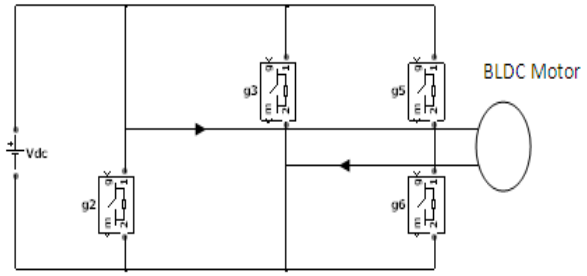

Fig. 5(b) Switching Action

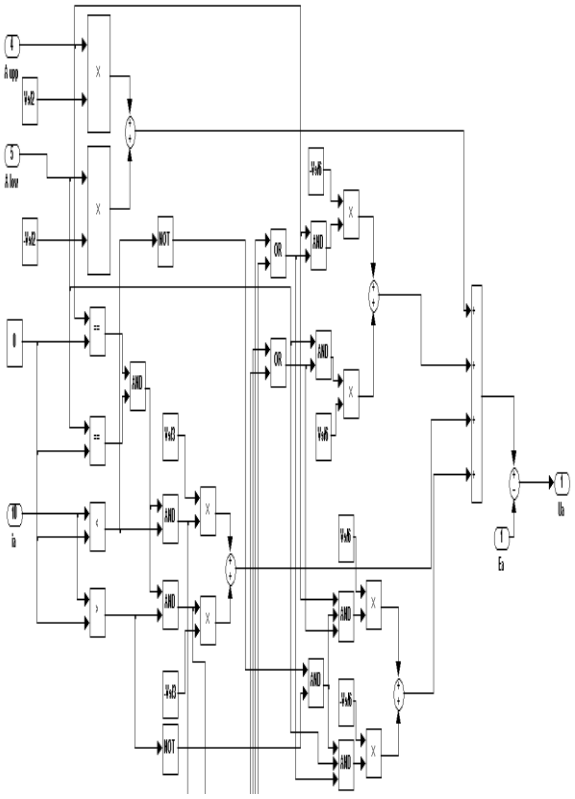

Fig. 6 Simulink model of inverter of Phase A

International Journal of Scientific & Engineering Research, Volume 3, Issue 12, December-2012
ISSN 2229-5518

2.3 Modeling Of Current Controller

Commutation means the process of switching current into different windings. It also depends on the PWM signal. The commutation logic is implemented through logic gates. The Current controller logic model which provides necessary gating signals for the inverter switches. The outputs are the driving signals for each switch in the inverter [12]. Current controller in Fig. 7 consists of PWM and Gating pulses. The position of the rotor is determined by testing every 60-degree intervals.

Commutation logic was developed by sensing the rotor positions. Hall sensors are positioned in such a way that as the rotor gets to the point, another arrangement of windings is energized and rotor is pulled around another 60 degree. After determining the rotor position, it starts giving the gating signals for the switches. The inverter is driven by means of six gating signals derived from the current controller. Table 1 shows the commutation switching sequence which accounts for the rotation of the rotor of BLDCM.

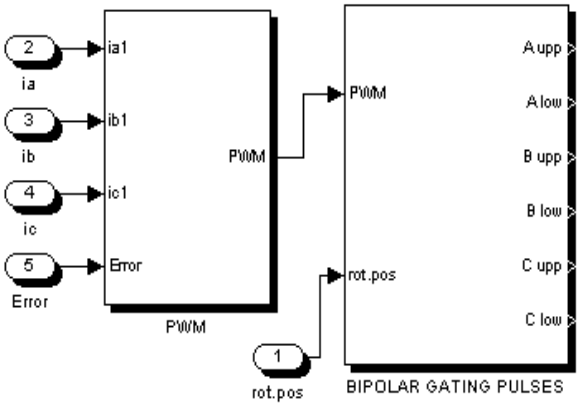

Fig. 7 Current Controller

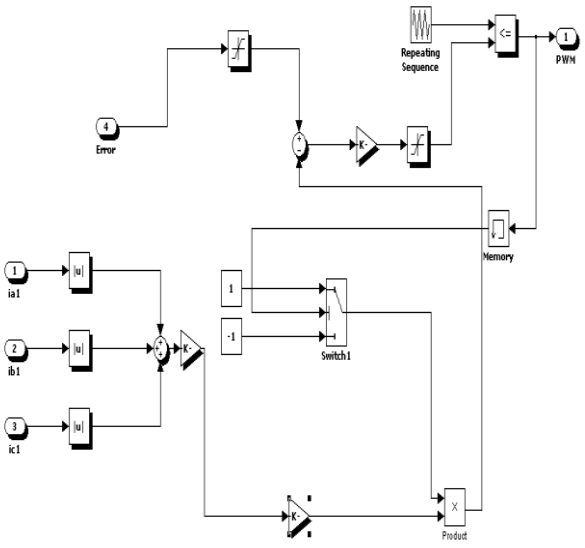

Fig. 8 PWM Generation

Fig. 8 illustrates the generation of PWM using a triangular wave. After determining the rotor position, it starts giving the gating signals for the switches. By this, a 120-degree conduction signal generator model is implemented. This model can generate exact square wave switching patterns. Commutation switching sequence in Table 1 consists of 3 upper switches and 3 lower switches named Au (upper), Al (lower), Bu (upper), Bl (lower), Cu (upper), Cl (lower) respectively. The table explains the switching sequence applied to each switch.

TABLE 1
COMMUTATION SWITCHING SEQUENCE

Rotor position	PWM	Au	Al	Bu	Bl	Cu	Cl
0-60	On	1	0	0	1	0	0
	Off	0	1	1	0	0	0
60-120	On	1	0	0	0	0	1
	Off	0	1	0	0	1	0
120-180	On	0	0	1	0	0	1
	Off	0	0	0	1	1	0
180-240	On	0	1	1	0	0	0
	Off	1	0	0	1	0	0
240-300	On	0	1	0	0	1	0
	Off	1	0	0	0	0	1
300-360	On	0	0	0	1	1	0
	Off	0	0	1	0	0	1

2.4 Modeling Of Position Controller

The recommended compensation for a position servo loop is provided by lag compensator in the forward path and rate filter in the feedback path. In Fig. 9 such a position controller is designed with lag and rate filter output. Lag compensator improves steady state error by increasing the low frequency gain without any resulting instability. It also increases the phase margin of the system to yield the transient response. By placing the lag transfer function in forward path makes the response fast and rate filter in the feedback path makes the oscillations damping. Thus the output settles in a considerable time. This results in the settling of output meaning launch vehicle reaching the target.

$$\text{Lag transfer function} = 0.67\frac{(s+10.8)}{(s+5)} \quad (11)$$

$$\text{Rate transfer function} = 26.8\frac{s}{s+142} \quad (12)$$

The transfer functions are experimentally proven within a set up. The error output is fed to the lag and feedback output is fed to the rate. Then the lag and rate is compared to obtain the current command to be provided to the current controller.

International Journal of Scientific & Engineering Research, Volume 3, Issue 12, December-2012
ISSN 2229-5518

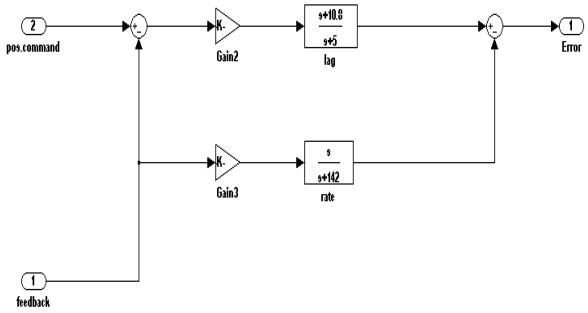

Fig. 9 Position Controller

2.5 Modeling Of Load Dynamics

From the angular position, linear motion of the ball screw actuator is detected. The rotatory motion is being transformed into linear motion. A deflection is obtained from this section. Nozzle dynamics is being modeled in state space analysis.

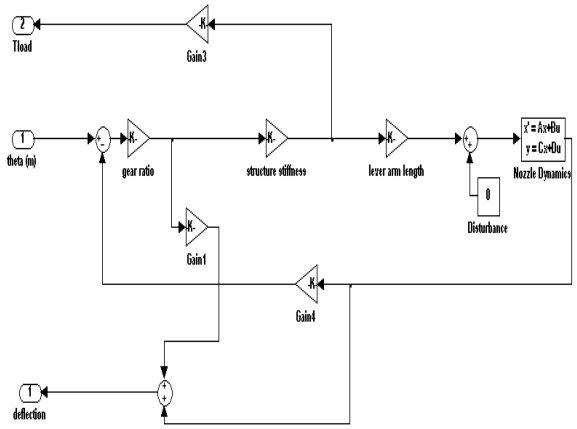

Fig. 10 Simulink of load dynamics

Load dynamics is implemented in Fig. 10. The deflection obtained from the actuator output is converted to voltage by means of a scale factor. This voltage is feedback to the position controller and compared with the position command signal to produce an error. This error signal accounts for the variation in position. Scale factor is assumed according to ratio of deflection and voltage. Fig. 11 is the overall Quadruplex BLDC motor based closed loop position servo system [7].Overall system is composed of Position controller, Current controller, Inverter, BLDC motor,Ball screw Actuator and Feedback Sensor. The Current controller, Inverter and BLDCM are of Quadruplex model.ie. these consist of four simplex arrangement placed in parallel.

3. Analysis of Failure Conditions

Failure conditions are analyzed by introducing an FDI Scheme in the position control system. The other objective of the work is to develop an electromechanical actuator (EMA) based position control system with redundancy technique. The highly redundant Electromechanical Actuation system comprises of a number of actuation elements controlled such that faults in individual elements are effectively detected, identified and isolated. The Dual Redundant Actuation System improves performance of the system during the occurrence of any system failure by providing a Dual Redundancy Both the chains have same type of control system. Only one chain works at a time, probably the main chain operates during normal condition of the system.

A new, simpler fault detection and isolation (FDI) technique is being developed, which will monitor the prime chain continuously. If any type of fault occurs in the prime chain, the FDI isolates the prime chain from the working system and switches to the redundant chain. Thereafter redundant chain will be driving the system. Another equivalent transfer function is implemented as a parallel path.

The equivalent transfer function is implemented by considering the feedback as an equivalent command signal. So the equivalent transfer function becomes the difference of lag and rate transfer functions. From the Fig. 12, equation can be written as

$$G(s) = \text{lag} - \text{rate}$$

$$G(s) = \frac{(s+15.81)(s+96.98)}{(s+5)(s+142)} \qquad (13)$$

Certain failure conditions are applied and outputs are analyzed. By verifying the difference of error obtained between the two different paths, the variations appearing when several failure conditions applied can be studied. Any deviation in the output of the system from the ideal output of the model determines the fault. Fig. 12 shows the FDI scheme implemented in simulink to detect the failures of the system. The dual redundancy in Electromechanical Actuation system provides better safety for launch vehicle actuation. Error difference obtained by applying several failure conditions are being plotted below. A simplest FDI scheme is implemented here by an equivalent transfer function.

International Journal of Scientific & Engineering Research, Volume 3, Issue 12, December-2012
ISSN 2229-5518

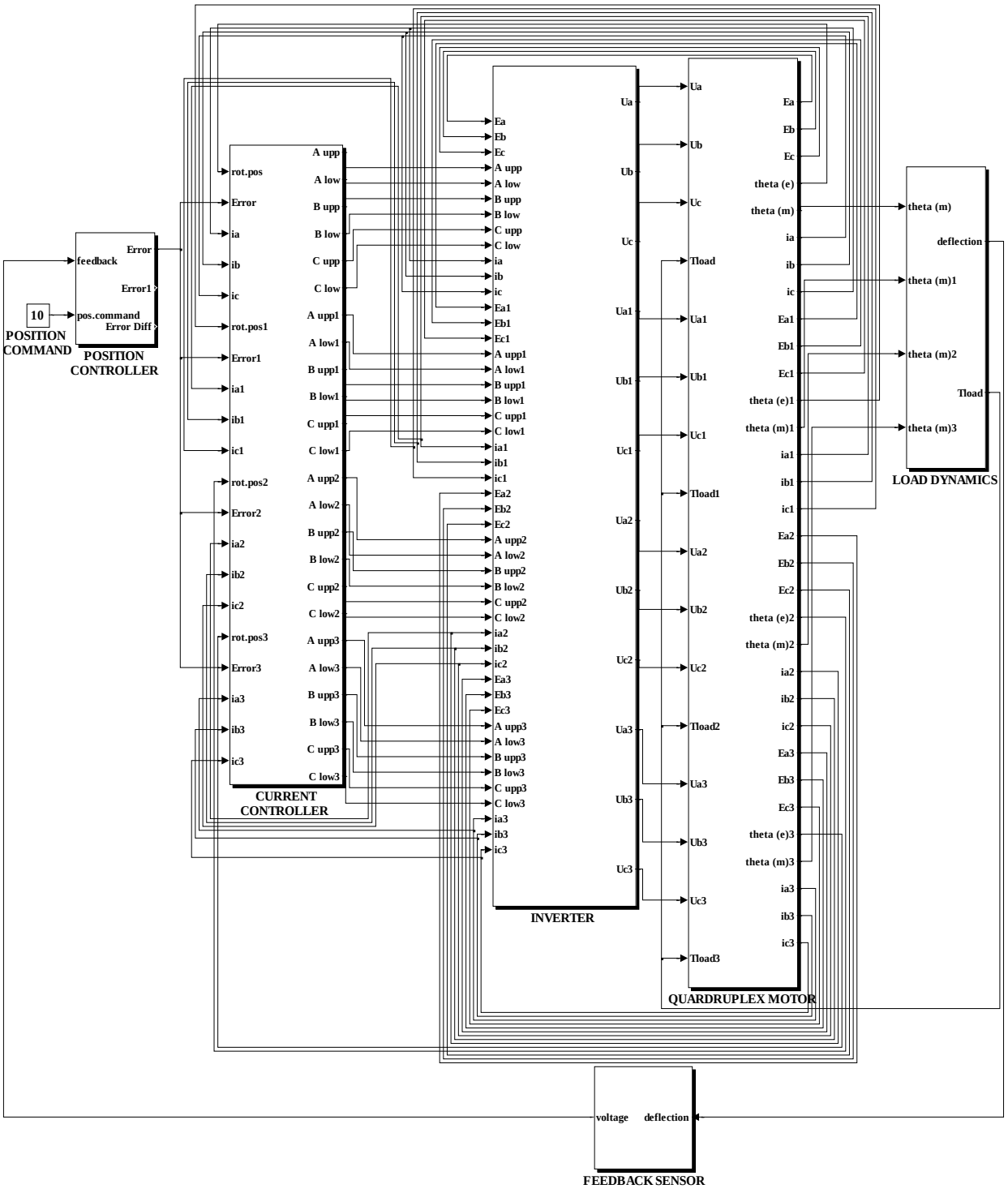

Fig. 11 Quadruplex BLDC Motor Based Position Servo System

International Journal of Scientific & Engineering Research, Volume 3, Issue 12, December-2012
ISSN 2229-5518

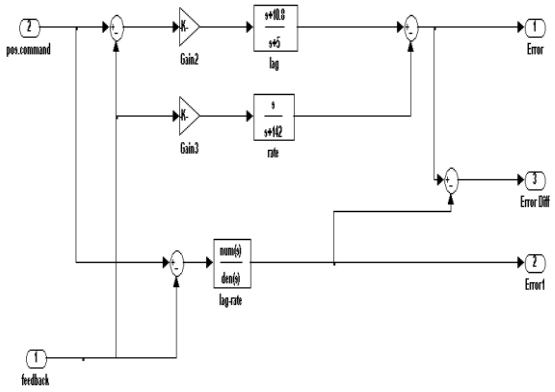

Fig. 12 Simulink model of FDI Scheme

4. Simulation Results and Discussions

According to the model of closed-loop control system for BLDCM mentioned above, some vital simulation works have been conducted. When three phase BLDCM is simulated, it generates Trapezoidal back EMF, Stator Currents and Theta. The inputs provided are Phase Voltages and Load Torque. During start up, the motor raises up slowly due to the initial inertia of rest. The motor back EMF also shows a similar variation initially since, the back EMF is directly proportional to speed [8].

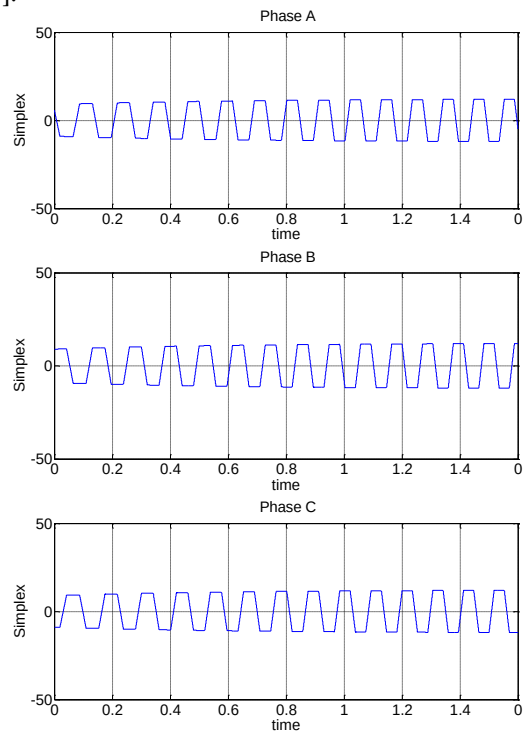

Fig. 13 Back EMF of three phases (Ea,Eb,Ec)

Fig. 13 three different phases of Back Emf is shown. The torque ripple in the waveform is due to the trapezoidal commutation provided. Torque ripple occurred is theoretically 13% for trapezoidal commutation.

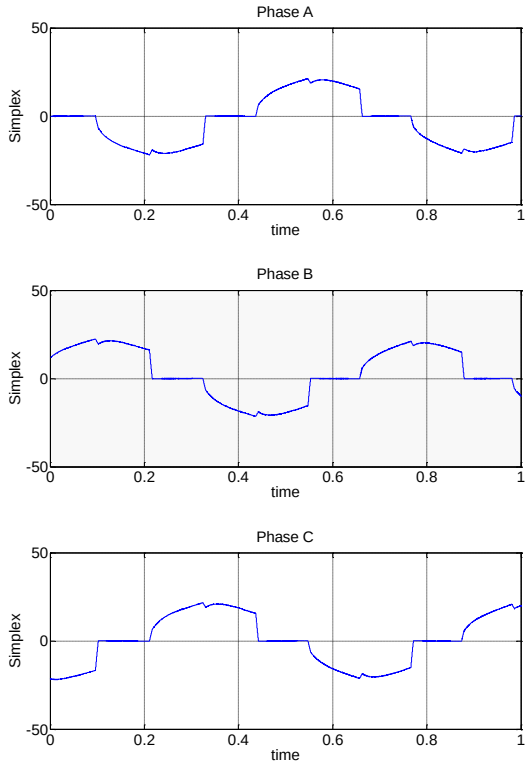

Fig. 14 Stator current of three phases (Ia,Ib,Ic)

In Fig. 14 three different phases of Stator currents are shown. Stator currents are also rectangular shaped, due to the trapezoidal commutation. By verifying the Back EMF and Stator Current waveforms, the modeling of BLDC Motor is verified.

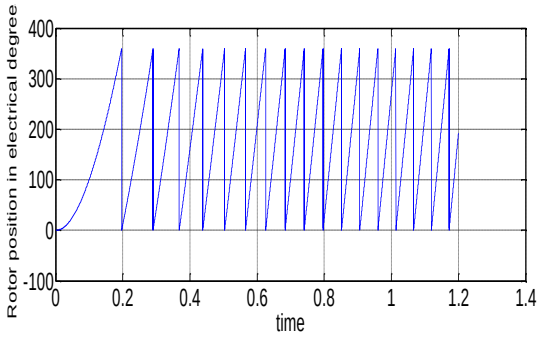

Fig. 15 Rotor Position

Rotor position expressed in electrical degrees is shown in Fig. 15. Phase Voltages are output of inverter which drives the BLDCM. The phase voltages are different for each phase which drives the motor. PWM signals control the commutation logic which accounts for the commutation. Six gating pulses are generated by the current controller and these are used to drive the power amplifier switches. Fig. 16 (shows the gating pulses for each upper and lower switches of three phases. As trapezoidal commutation is designed, only two phases out of three phases will be active at a time. This is advantageous compared to the sinusoidal commutation.

International Journal of Scientific & Engineering Research, Volume 3, Issue 12, December-2012
ISSN 2229-5518

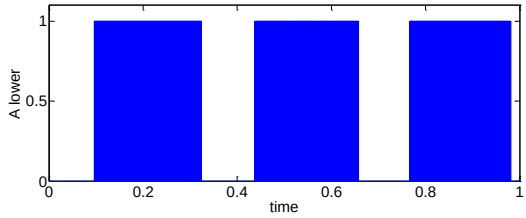

Fig. 16(a) Gating signal for lower switch of phase A

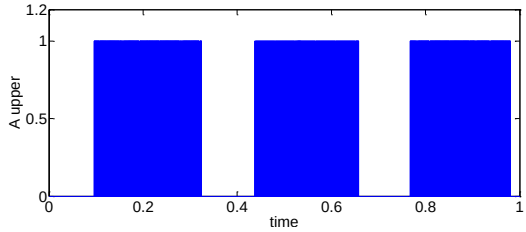

Fig. 16(b) Gating signal for upper switch of phase A

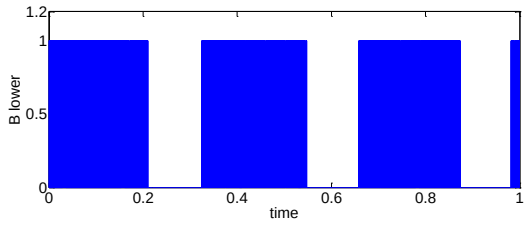

Fig. 16(c) Gating signal for lower switch of phase B

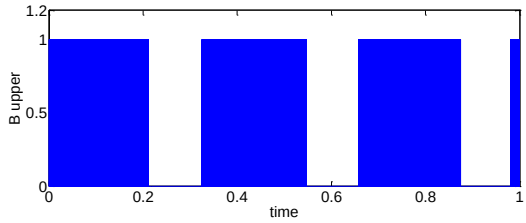

Fig. 16(d) Gating signal for upper switch of phase B

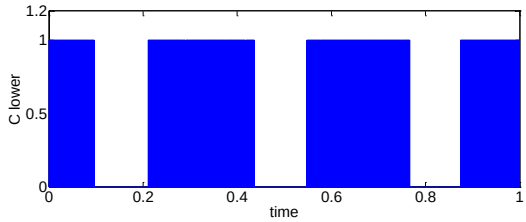

Fig. 16(e) Gating signal for lower switch of phase C

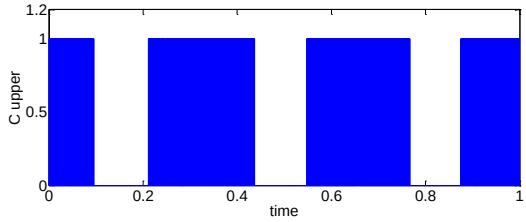

Fig. 16(f) Gating signal for upper switch of phase C

Fig. 16 Gating signals

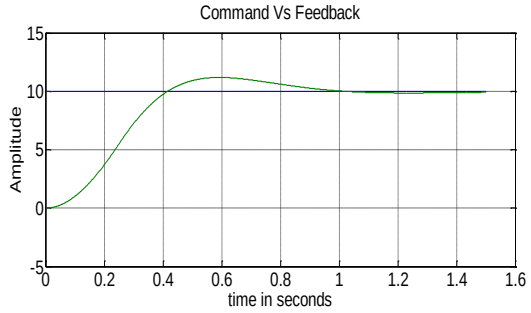

Fig. 17 Command Versus Feedback

Command - feedback is shown in Fig. 17.This explains that the feedback signal will settle to the command signal after certain time, indicating the output of position controller. These are the results obtained by simulating a normal position servo system and an equivalent transfer function and error difference between them is found out.

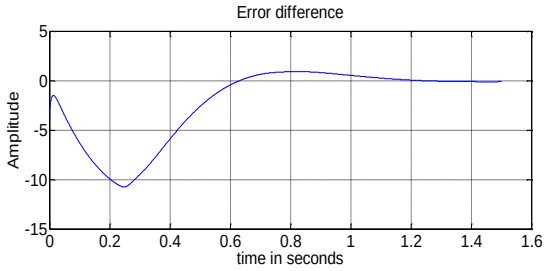

Fig. 18(a) Difference between Normal and FDI system

Fig. 18(b) Application of positive bias to the feedback

Fig. 18(c) Application of negative bias to the feedback

Fig. 18(d) Constant of lag is increased

International Journal of Scientific & Engineering Research, Volume 3, Issue 12, December-2012
ISSN 2229-5518

Fig. 18(e) Change in pole value

Fig. 18(f) Constant of lag changed to a negative value

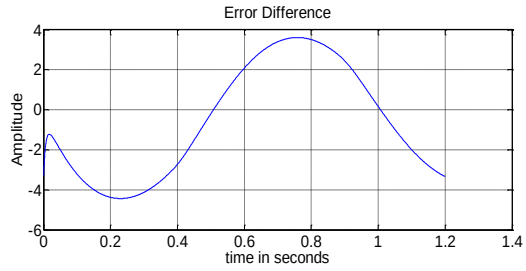

Fig. 18(g) Change in constant of rate filter

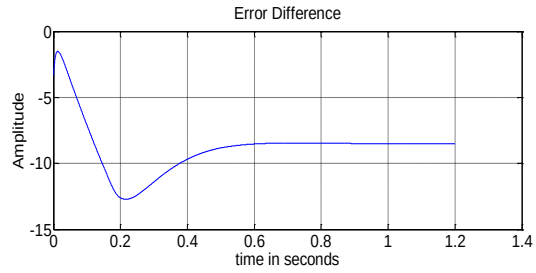

Fig. 18(h) Change in pole value of rate filter.

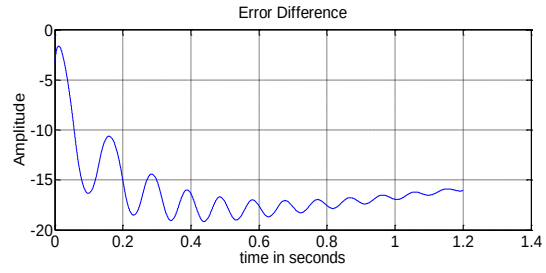

Fig. 18(i) Change in zero value of rate filter.

In Fig. 18(a) Error comparison between actual working system and an equivalent transfer function relating actual system is found to be a zero error. They are approximately equal. In Fig. 18(b) when a positive bias is applied to the feedback of the normal system, it is found that the error difference is slightly less than zero. ie. The outputs never settle down. Fig. 18(c) shows the result when a negative bias is applied to the feedback of the normal system. Here it is viewed that the error difference is slightly greater than zero. In Fig. 18(d) when constant of lag is increased, result shows that the two systems never match. An error always occurs. In Fig. 18(e) pole value is changed to indicate another fault has occurred in the normal system. Fault can be easily identified by viewing the result. Fig. 18(f) shows that the error difference goes on decreasing when constant of lag is changed to a negative value. In Fig. 18(g) when constant of rate is increased, result shows that the two systems never match. An error always occurs. Result when pole value of rate filter is changed is shown in Fig. 18(h).Here error difference becomes constant. In Fig. 18(i) an oscillatory response obtained so that the error difference between them will never become zero. Failure conditions are noted by viewing that the error difference between the normal system and FDI system is always non zero.

5. Conclusion

An electromechanical actuator based closed loop position servo system and certain failure conditions are detected by introducing an FDI scheme has been modeled. The simulation results are presented. Based on the mathematical model of the BLDCM, the modeling and simulation of the control system are presented in this study. The simulation results demonstrate that the simulated waveforms fit theoretical analysis well. The control system can operate stably and has the fairly good dynamic and static characteristics. Also eight different failure conditions are analyzed with the help of FDI scheme. This is simulated in order to view the results.

TABLE 2
BLDC MOTOR SPECIFICATIONS

Parameters	**Specification**
Stator Connection	Y connected
Power	1.7KW
Resistance / Phase, R	0.5 Ω
Self Inductance / Phase, L	0.0013H
Mutual Inductance/ Phase, M	0
Pole Pairs, P	8
Supply Voltage, Vdc	50V
Back EMF constant	0.6V/rad
Rotor Moment of Inertia, J	0.2156Kg/m^2
Rotor Friction Constant, B	0.2Nm/rad/s

International Journal of Scientific & Engineering Research, Volume 3, Issue 12, December-2012
ISSN 2229-5518

REFERENCES

[1]. Vinatha U, Sweta Pola, Dr.K.P.Vittal (2008) *"Simulation of Four Quadrant Operation & Speed Control of BLDC Motor on Matlab / Simulink"*. IEEE Region '10 Conference TENCON.

[2]. Ma Ruiquing, Liu Weiguo, Luo Guangzhao,Hu Yashan (2005) *"The Balanced Current Control of Dual-Redundancy Permanent Magnetic Brushless DC Motor"*. 8th International Conference on Electrical Machines and Systems.

[3]. A.Halvaei Niasar, H. Moghbelli, A.Vahedi (2009) *"Modeling, Simulation and Implementation of Four -Switch, Brushless DC motor Drive based on switching functions."* IEEE Conference, EUROCON.

[4]. D.Krkljes, C.Morvai, K.Babkovic, L.Nagy (2010) *"BLDC Motor Driver – Development of Control and Power Electronics"*.7th International Conference on Microelectronics Proceedings (MIEL).

[5]. Yongxiang Xu, Yu Tang, Junwei Zhu, Jibin Zou, Changjun Ma (2008) *"Control of a BLDC Motor for Electromechanical Actuator"*. International Conference on Electrical Machines and Systems ICEMS.

[6]. Kaiping Yu, Hong Guo, Dayu Wang, Lanfeng Li (2008) *"Design of Position Servo-System of BLDCM Based on Frequency Domain Method"*. International Conference on Electrical Machines and Systems ICEMS.

[7]. Hong Guo, Wei Wang, Wei Xing, Yanming Li (2008) *"Design and Research on Electrical/Mechanical Hybrid Four-Redundancy Brushless DC Motor System"*. IEEE Conference on Vehicle Power and Propulsion Conference VPPC, Harbin, China.

[8]. Anas S.R, Hemanth Jaison, Anish Gopinath, M.N Namboothiripad, M.P.Nandakumar (2011) *"Modeling and Simulation Analysis of a Redundant Electromechanical Actuator based Position Servo System"*. International Conference on Computer, Communication and Electrical Technology ICCCET.

[9]. Salaheddin A, Zabalawi, Adel Nasiri (2007) *"State Space Modeling and Simulation of Sensor less Control of Brushless DC Motors Using Instantaneous Rotor Position Tracking"*. IEEE Conference on Vehicle Power and Propulsion Conference VPPC.

[10]. G.H.Jang, C.I.Lee (2005) *"Dual Winding Method of a BLDC Motor for Large Starting Torque and High Speed"*. IEEE Transactions On Magnetics Vol.41, No-10.

[11]. Pragasen Pillay, Ramu Krishnan (1989) *"Modeling, Simulation, and Analysis of Permanent-Magnet Motor Drives, Part II: The Brushless DC Motor Drive"*. IEEE Transactions on Industry Applications Vol: 25, No-2.

[12]. Dr. Ron J. Patton, Mr. J. Chen, (1993) "*Advances in Fault Diagnosis using Analytical Redundancy*". Department of Electronics, University of York, YO1 5DD.

[13]. Inseok Hwang, Sungwan Kim, Senior Member, IEEE, Youdan Kim, Member, IEEE, and Chze Eng Seah, (2010) "*A Survey of Fault Detection, Isolation, and Reconfiguration Methods*". IEEE Transaction on control system technology, vol. 18, No. 3.

[14]. Janos J. Gertler, (1986) "*Survey of Model-Based Failure Detection and Isolation in Complex Plants*". Presented at the IFAC Symposium on Microcomputer Applications to Process Control, Istanbul, Turkey, and published in Vol. 7 of the IFAC Proceedings Series, 1987, IEEE

[15]. Edward Balaban, Abhinav Saxena, Prasun Bansal, Kai F. Goebel, Paul Stoelting, Simon Curran (2009) *"A Diagnostic Approach for Electro-Mechanical Actuators in Aerospace Systems"* ©2009 IEEE.

[16]. W. Chen and M. Saif (2007) "*Observer based strategies for actuator fault detection, isolation and estimation for certain class of uncertain nonlinear systems*" IET Control Theory Appl., 2007, 1, (6), pp. 1672–1680

[17]. A. Garcia, I. Cusid6, J.A. Rosero, J.A. Ortega, L. Romeral(2008) "*Reliable Electro-mechanical Actuators in Aircraft*" IEEE A&E Systems Magazine.

[18] D D .Dhawale, J.G.Chaudhari, Dr.M.V.Aware (2010) "*Position control of four switch three phase BLDC motor using PWM control*" Third International Conference on Emerging Trends in Engineering and Technology © 2010 IEEE

[19]. Shiyoung Lee, Tom Lemley(2009) "*A Comparison study of the commutation methods for the three phase permanent magnet brushless DC Motor*"

[20]. Fernando Rodriguez, Ali Emadi (2007) "*A Novel digital control technique for Brushless Motor drives*" IEEE Transactions on Industrial Electtronics, VOL. 54, NO. 5